Article

Twisted 8-Acyl-1-dialkyl-amino-naphthalenes Emit from a Planar Intramolecular Charge Transfer Excited State

Christopher Abelt [1],* and Kirsten Sweigart [2]

[1] Department of Chemistry, College of William and Mary, Williamsburg, VA 23185, USA
[2] Independent Researcher, Northbrook, IL 60062, USA; kmsweigart@outlook.com
* Correspondence: cjabel@wm.edu

Abstract: Fluorescence from dialkylamino donor–acyl acceptor substituted 1,8-naphthalene derivatives can occur either from a planar (PICT) or a twisted (TICT) intramolecular charge transfer excited state. The photophysical properties of 8-acetyl-1-(dimethyl-amino)naphthalene (**3**) and 8-pivaloyl-1-(dimethyl-amino)naphthalene (**4**) are compared with 1-methyl-2,3-dihydronaphtho[1,8-bc]azepin-4(1H)-one (**5**). In **3** and **4**, both the carbonyl and amino groups are forced to twist out of the plane of the naphthalene ring. In **5**, these groups are nearly coplanar with the naphthalene. Neither **3** nor **4** fluoresce as strongly as **5**, but all three show similar degrees of solvato-chromism and all are strongly quenched by alcohol solvents. Nitrile **6**, 8-cyano-1-(dimethyl-amino)naphthalene, does not show the same degree of solvato-chromism as **3–5**, nor is it as affected by alcohols. Calculations corroborate the experimental results, indicating that **3–5** emit from a PICT excited state.

Keywords: solvato-chromism; charge transfer; PICT; TICT; peri

1. Introduction

Prodan (**1**, 6-propionyl-2-(dimethyl-amino)naphthalene, Figure 1) is a highly fluorescent molecule that emits from an intramolecular charge transfer (ICT) excited state [1]. Because the excited state dipole moment is nearly twice as large as the ground state, 2,6-Prodan exhibits significant solvato-chromism [2–5]. Similar behavior is observed with the 1,5-regioisomer [6–8]. In these compounds, both the dimethyl-amino and carbonyl groups are free to rotate out of the plane of the naphthalene ring in the excited state, potentially creating a large degree of charge separation.
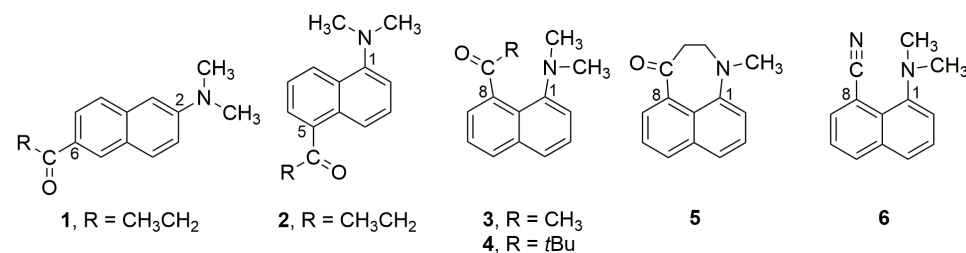

Figure 1. Structures of Prodan derivatives **1–6**.

Several donor-acceptor substituted fluorophores possessing a dialkylamino group as the donor are thought to form twisted intramolecular charge transfer (TICT) excited states [9–11]. Of these compounds, dimethyl-amino-benzonitrile (DMABN, **7**, Figure 2) is archetypical. Excitation of DMABN initially gives a planar, locally excited (LE) state. Geometrical twisting about the C-N bond gives rise to a surface crossing to a TICT excited state. Because the nitrogen *n*-orbital is orthogonal to the π-system, there is nearly complete electron transfer from the nitrogen to the benzonitrile group. Related model compounds corroborate this hypothesis: the planar model **8** shows only LE emission, while the twisted

model **9** shows only red-shifted charge transfer emission (Figure 2) [12–16]. In contrast, we have found that both the 2,6- and 1,5-Prodan derivatives in which the dialkyl-amino groups are constrained to be co-planar behave similarly to the parent compounds, suggesting that the excited states are planar (PICT) and not twisted (TICT) [17–21].
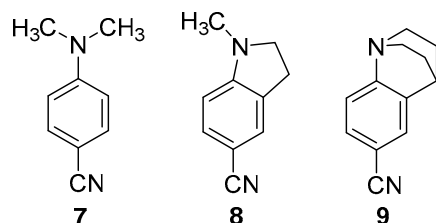

Figure 2. Structures of DMABN, **7**, and its planar (**8**) and twisted (**9**) model compounds.

Several 1,8-derivatives of Prodan have been reported by Kiefl and co-workers [22]. With donor-acceptor substituted 1,8-naphthalenes, the *peri*-interaction between the two groups forces them to twist out of the plane in the ground state [23–27]. With dimethyl-amino donors, the nitrogen atom is pyramidal and its lone pair is directed toward the carbonyl, resulting in a small separation between the nitrogen and the carbonyl carbon (~2.7Å). Kiefl also reported that 1,8-Prodan derivatives exhibited anomalous Stokes shifts. We wondered whether the geometrical constraints in these compounds would favor the formation of TICT excited states, as suggested by Kiefl. We examined this hypothesis by comparing the photophysical behavior of **5**, where the amino and carbonyl groups are constrained in a ring, with **3**, **4**, and **6** (Figure 1).

2. Materials and Methods

Nuclear magnetic resonance spectra were obtained with an Agilent DD2-400 spectrometer. Reagents were obtained from Acros Organics or Sigma-Aldrich unless otherwise indicated. Butyl nitrite was prepared as described [28]. Cuprous cyanide was prepared from $CuSO_4$ and $NaHSO_3$ as described [29]. All solvents used for absorption and fluorescence were spectrophotometric grade. Absorption and fluorescence data were collected using a fiber optic system with an Ocean Optics Maya CCD detector using a miniature deuterium/tungsten lamp and a 365 nm LED light source, respectively. Cuvettes were thermostated at 23 °C for fluorescence studies. Emission intensities were processed by subtracting the electronic noise, converting wavelengths to wavenumbers, multiplying by $\lambda^2/\lambda_{max}^2$ to account for the effect of the abscissa-scale transformation [30], and dividing by the spectral response of the Hamamatsu S10420 CCD. Relative quantum yields were determined using anthracene as the reference (Φ = 0.30).

Electronic structure calculations were carried out using Gaussian 16 [31]. Ground state geometries were optimized using the DFT B3YLP method with the 6-311G + (2d,p) basis set. Excited states were optimized using the TD-SCF DFT B3LYP method with the 6-311G + (2d,p) basis set and the dihedral angle scan was carried out with the 6-31G + (d) basis set. Solvent effects were modeled with the IEFPCM method.

The syntheses of **3**–**6** (Scheme 1) followed reported procedures with some slight modifications. Compound **3** was prepared by the method of Kirby and Percy [32]. Compound **4**, originally made via the organo-manganese derivative [33], was made by treating the organolithium intermediate **13** with pivaloyl chloride. The preparation of **5** starting from 1-naphthol (**10**) was reported as an intermediate in the synthesis of a Dansyl derivative [34]. Nitrile **6** was prepared following Kiefl's procedure [22] using methyl iodide in place of dimethyl sulfate for the methylation of the amine **17** and dimethyl acetamide instead of dimethyl formamide as the solvent in the cyanation (**18**→**6**). All final products (**3**–**6**) gave NMR spectra consistent with published values.
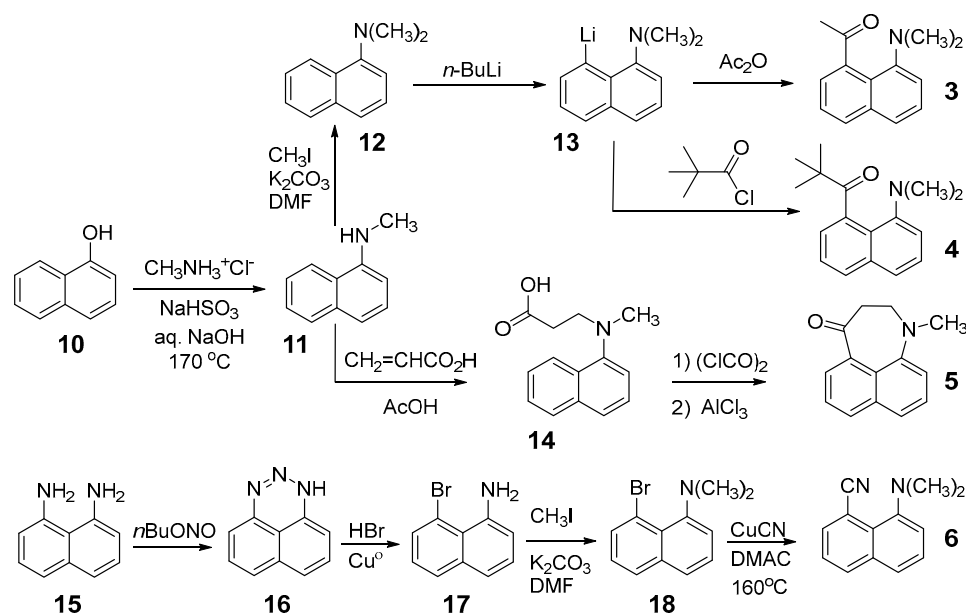
Scheme 1. Preparation of **3–6**.

2.1. 1-(Methylamino)naphthalene (**11**)

A steel autoclave was charged with 1-naphthol (**10**, 10.0 g, 69.4 mmol), sodium bisulfite (16.5 g, 159 mmol), and methylamine hydrochloride (15.5 g, 230 mmol) followed by a solution of aq. NaOH (5.6 M, 40 mL, 225 mmol). The autoclave was sealed with a Teflon-wrapped stainless-steel o-ring and heated to 163 °C overnight with stirring. The reaction was allowed to cool, the contents were removed with suction, and the vessel was washed with water and acetone. The washings were combined with the reaction contents, NaCl (40 g) was added, and the mixture was stirred overnight to allow the acetone to evaporate. The resulting solid was filtered with suction and air-dried overnight. The solid was stirred in CH_2Cl_2 (50 mL) and the mixture was filtered. The solid residue was stirred in CH_2Cl_2 (50 mL) and filtered. The combined filtrates were diluted with hexanes (150 mL). The organic phase was washed with 1 M NaOH (4 × 60 mL) to remove unreacted naphthol and then with water (150 mL). The organic layer was dried over $CaCl_2$, filtered, and concentrated in vacuo. The residue was distilled under vacuum (0.25 torr, b.p. 165 °C) giving the methylamine **11** (7.70 g, 49.0 mmol, 71%).

2.2. 1-(Dimethylamino)naphthalene (**12**)

1-(Methylamino)-naphthalene (**11**, 3.6 g, 23 mmol) and K_2CO_3 (5.0 g, 36 mmol) were stirred together in DMF (25 mL). Methyl iodide (5.5 g, 38 mmol) was added and the reaction was stirred at room temperature overnight. The reaction was filtered and the inorganic salts were washed with acetone. The filtrate was diluted with CH_2Cl_2 (100 mL) and hexanes (200 mL) and washed with water (5 × 100 mL). The organic phase was dried over $CaCl_2$, filtered, and concentrated in vacuo. The residue was distilled under vacuum (0.25 torr), giving **12** (2.5 g, 15 mmol, 65%).

2.3. 1-Acetyl-(8-dimethylamino)naphthalene (**3**)

Dimethyl-amino-naphthalene **12** (2.0 g, 11.7 mmol) was dissolved in Et_2O (30 mL) under N_2. A 2.5 M solution of *n*-BuLi in hexanes (19 mL, 47.5 mmol) was added quickly. The solution gradually became dark and was stirred slowly for 4 days. Stirring was stopped and the lithium salt was allowed to settle. Most of the Et_2O was removed with suction through a glass wool-packed pipet. More Et_2O (10 mL) was added, the mixture was stirred for 1 min, the lithium salt was allowed to settle, and most of the Et_2O was removed as above. The salt was washed again as above. Et_2O (30 mL) was added and the reaction was cooled in a dry ice-acetone bath. A solution of freshly distilled acetic anhydride

(1.5 g, 14.7 mmol) in Et$_2$O (20 mL) was added dropwise and the reaction was allowed to warm to room temperature overnight with stirring. Methanol was added and the solution was concentrated in vacuo. The residue was extracted with CH$_2$Cl$_2$ (3 × 50 mL), and the combined extracts were washed with brine (3 × 50 mL), dried over MgSO$_4$, and concentrated in vacuo. Compound **3** (480 mg, 19%) was isolated from the resulting oil (~1.2 g) by column chromatography on silica gel with a gradient elution (0→25% ethyl acetate in hexanes).

2.4. 1-Pivaloyl-(8-dimethylamino)naphthalene (**4**)

Dimethyl-amino-naphthalene **12** (1.0 g, 5.85 mmol) was dissolved in Et$_2$O (15 mL) under N$_2$. A 1.6 M solution of *n*-BuLi in hexanes (15 mL, 24 mmol) was added quickly. The solution became dark and was stirred slowly for 6 days, over which time the Et$_2$O evaporated. More Et$_2$O (20 mL) was added and the solid was washed twice with Et$_2$O as above. Et$_2$O (20 mL) was added and the reaction was cooled in a dry ice-acetone bath. A solution of freshly distilled pivaloyl chloride (1.0 g, 8.3 mmol) in Et$_2$O (10 mL) was added dropwise and the reaction was allowed to warm to room temperature over several hours with stirring. The mixture was poured into water (100 mL), Et$_2$O (100 mL) was added, and the layers were shaken together and separated. The organic phase was washed with brine (100 mL), dried over Na$_2$SO$_4$, and concentrated in vacuo. Column chromatography of the residue on silica gel with a gradient elution (0→10% ethyl acetate in hexanes) gave 360 mg of a 4:1 mixture of **4** and **12**. This mixture was dissolved in hexanes (100 mL), washed with 1 M HCl (3 × 75 mL), dried over Na$_2$SO$_4$, filtered, and concentrated in vacuo giving **4** (260 mg, 1.02 mmol, 17%).

2.5. 3-(Methyl(naphthalen-1-yl)amino)propanoic Acid (**14**)

Commercial acrylic was distilled under vacuum (0.25 torr) before use. 1-(Methylamino) naphthalene **11** (7.4 g, 47.1 mmol) and acrylic acid (14.37 g, 199 mmol) were combined and heated to 70 °C for 2 h under a CaCl$_2$ drying tube. Excess acrylic acid (9.24 g) was removed by vacuum distillation (0.25 torr) and the residue was kept under vacuum overnight. NMR analysis showed that 5% acrylic acid and 3% acrylic acid dimer remained. This product was used without further purification.

2.6. 1-Methyl-2,3-dihydronaphtho[1,8-bc]azepin-4(1H)-one (**5**)

The crude product above was dissolved in CH$_2$Cl$_2$ (50 mL), 10 drops of DMF were added and the solution was cooled in an ice-water bath under a CaCl$_2$ drying tube. A solution of oxalyl chloride (7.5 g, 59.1 mmol) in CH$_2$Cl$_2$ (20 mL) was added dropwise and the reaction was stirred for 1 h. The solvent was removed in vacuo, and the residue was dried under vacuum (0.25 torr) for 1.5 h. The residue was dissolved in CH$_2$Cl$_2$ (40 mL) and added dropwise to a slurry of AlCl$_3$ (8.13 g, 61.0 mmol) in CH$_2$Cl$_2$ (40 mL) in an oil bath heated to 55 °C. The reaction was stirred at 55 °C for 1.5 h. The reaction was cooled in an ice-water bath, brine (~3 mL) was added dropwise, and the mixture was stirred for 3 days. The mixture was filtered with suction and the solids were washed with CH$_2$Cl$_2$ until the filtrate was clear (~125 mL total). The filtrate was diluted with hexanes (150 mL), washed with 1 M NaOH (4 × 35 mL), water (100 mL), dried over Na$_2$SO$_4$, filtered, and concentrated in vacuo. The residue was sublimed under vacuum (0.25 torr) giving **5** (2.77g, 13.1 mmol, 28% from **14**). Compound **5** (1.75 g) was purified further by recrystallization from hexanes (80 mL) and CH$_2$Cl$_2$ (2 mL) giving 1.3 g after washing with cold hexanes and air-drying.

2.7. 1H-naphtho[1,8-de][1,2,3]triazine (**16**)

1,8-Diaminonaphthalene (**15**, 5.25 g, 33.2 mmol) was dissolved in ethanol (50 mL) and acetic acid (10 mL) and the mixture was cooled to 15 °C. *n*-Butyl nitrite (4.4 mL, 37.6 mmol) was added dropwise and the reaction was stirred overnight. The resulting solid was collected with suction and washed with water until the filtrate was colorless. The

solid was air-dried for 1 h giving 5.6 g of crude **16** as a brown solid. It was used without further purification.

2.8. 1-Amino-8-bromonaphthalene (**17**)

Copper powder (1.46 g, 23 mmol) was activated by washing twice with a solution of iodine (1 g) in acetone (50 mL) and three times with a 1:1 mixture of acetone and concentrated aq. HCl (33 mL). The bright red powder was dried under a stream of N_2 gas. Crude **16** above was added to concentrated aq. HBr (35 mL) and the mixture was immersed in an oil bath heated to 85 °C. The copper powder was added slowly in portions causing the solution to bubble and form a black char. The bubbling subsided in a few minutes, and heating was maintained for 15 min. The reaction was removed from the oil bath and stirred overnight. Water (70 mL) was added and the mixture was brought to a boil and filtered with suction. The solid was collected and boiled in fresh water (50 mL). This step was repeated. The filtrates were combined, cooled, and neutralized with conc. aq. NH_4OH (40 mL, pH~11). The aqueous layer was extracted with CH_2Cl_2 (3 × 75 mL). The combined organic extracts were washed with water (2 × 200 mL), dried over $CaCl_2$, and concentrated in vacuo. The residue was distilled under vacuum (0.25 torr) giving **17** (3.31 g, 15 mmol, 45% from **16**).

2.9. 1-(Dimethylamino)-8-bromonaphthalene (**18**)

An Ace-Thred glass pressure tube was charged with **17** (1.65 g, 7.43 mmol), K_2CO_3 (4.0 g, 29 mmol), and DMF (20 mL). Methyl iodide (6.25 g, 44 mmol) was added, and the tube was sealed with a PTFE plug with an FETFE o-ring. It was heated to 70 °C for two days. After cooling to room temperature, the mixture was filtered with suction to remove the inorganic salts. The filtrate was distilled under vacuum (0.25 torr) at 60 °C to remove the DMF. The residue was taken up in CH_2Cl_2, filtered, and concentrated in vacuo. The residue was distilled under vacuum (0.25 torr) giving **18** (1.68 g, 6.72 mmol, 90%).

2.10. 1-Cyano-8-(dimethylamino)naphthalene (**6**)

CuCN (720 mg, 8.0 mmol) and **18** (1.48 g, 5.9 mmol) were stirred together in freshly distilled DMAC (13 mL) and the mixture was heated to reflux under Ar for 4 h. DMAC was removed by vacuum distillation at 75 °C. Water (3.6 mL) was added to the residue followed by $FeCl_3 \bullet 6H_2O$ (4 g, 14.8 mmol) and conc. HCl (0.8 mL) and the mixture was stirred at 70 °C for 30 min. The contents were diluted with water (200 mL) and the aqueous layer was extracted with CH_2Cl_2 (4 × 50 mL), The combined organic layers were washed with water (3 × 200 mL), dried over $CaCl_2$, filtered, and concentrated in vacuo. The residue was distilled under vacuum (0.25 torr) giving **6** (520 mg, 2.6 mmol, 44%). Compound **6** was purified further by column chromatography on silica gel with a gradient elution (0→20% ethyl acetate in hexanes).

3. Results

3.1. Photophysical Studies

3.1.1. Absorption

Kiefl reported that the absorption maxima of **3** and **6** in methanol are 300 and 340 nm, respectively [22]. We found that the long-wavelength absorption maxima for **3–5** are at 304 ± 3, 303 ± 3, and 345 nm ± 1, respectively, over a series of solvents ranging from apolar, aprotic to polar, protic (toluene, dichloromethane, acetone, and ethanol). For **3** and **4**, the absorption maxima were shifted to shorter wavelengths with the protic solvent ethanol and this shift accounted for the slightly wider range of absorption maxima relative to **5**. The nitrile **6** absorbs at longer wavelengths (λ_{max} = 348 nm in toluene).

3.1.2. Fluorescence

Azepinone **5** and nitrile **6** fluoresce strongly compared with **3** and **4** (Table 1). For all compounds, the strongest fluorescence is in an apolar, aprotic solvent. All show decreased

emission as the solvent polarity increases. However, the relative decrease for **6** is only a factor of three, whereas **5** decreases by nearly eight. Compounds **3** and **4** remain weakly fluorescent in polar, aprotic solvents. The decrease of the fluorescence quantum yield with increasing solvent polarity has been attributed to the smaller energy gap between the ground and excited states in these ICT systems, which enhances non-radiative deactivation [17,18]. The fluorescence spectra of **3**–**6** in various solvents are shown in Figure 3.

Table 1. Fluorescence properties of **3**–**6**.

Solvent [a]	3		4		5		6	
	Φ_f $\times 10^{-2}$	λ_{em} (nm)	Φ_f $\times 10^{-2}$	λ_{em} (nm)	Φ_f $\times 10^{-2}$	λ_{em} (nm)	Φ_f $\times 10^{-2}$	λ_{em} (nm)
Cyc	6.8	502	1.1	487	21.5	500	55.5	464
Tol	7.9	538	3.0	520	37.0	539	43.2	491
PhCl	7.3	558	3.8	532	23.6	559	54.4	480
CH_2Cl_2	4.5	583	3.2	554	16.5	583	45.8	508
EtOAc	4.0	560	1.9	535	6.3	566	24.5	508
Et_2O	1.4	566	0.6	531	9.9	566	36.6	496
Me_2CO	2.0	585	1.4	556	8.8	583	22.3	522
MeCN	1.5	603	1.3	567	5.6	598	22.5	529
DMSO	1.5	612	1.6	576	4.7	607	18.7	542
*i*PrOH	0.1	636	- [b]	- [b]	0.6	637	28.8	524

[a] Solvents are cyclohexane, toluene, chlorobenzene, dichloromethane, ethyl acetate, diethyl ether, acetone, acetonitrile, dimethyl sulfoxide, and isopropanol. [b] Not observed.
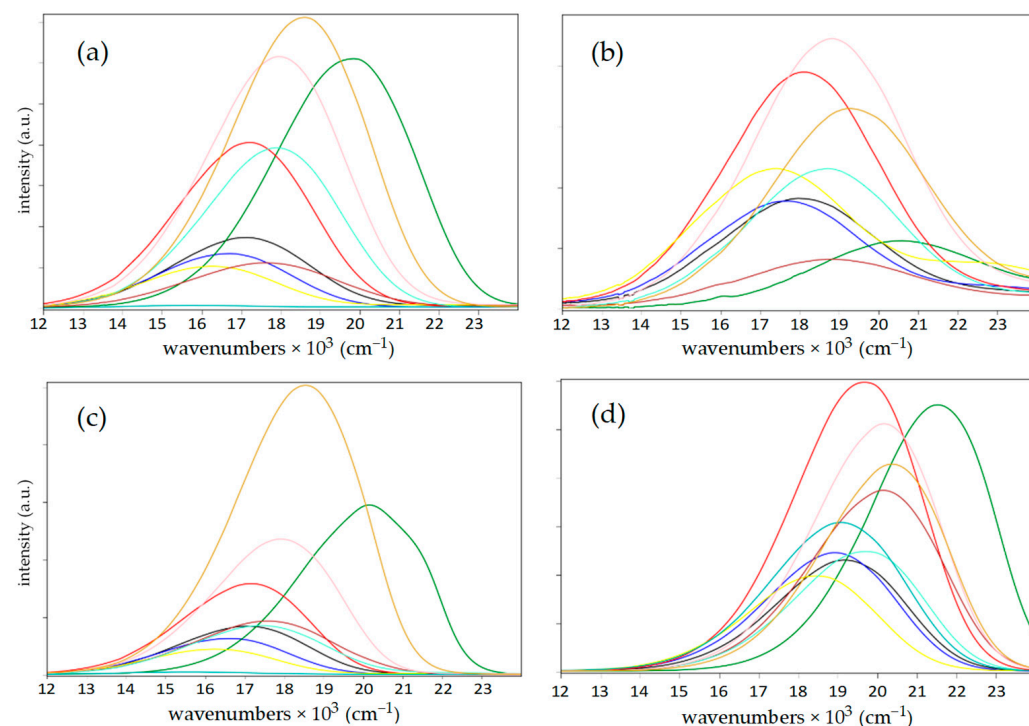

Figure 3. Fluorescence spectra of (**a**) 1.6×10^{-5} M **3**, (**b**) 1.0×10^{-4} M **4**, (**c**) 2.2×10^{-5} M **5**, and (**d**) 1.7×10^{-5} M **6** in various solvents: ■ cyclohexane, ■ toluene, ■ chlorobenzene, ■ methylene chloride, ■ ethyl acetate, ■ diethyl ether, ■ acetone, ■ acetonitrile, ■ dimethyl sulfoxide, and ■ isopropanol (except for **b**). Excitation at 365 nm.

Unlike **6**, ketones **3**–**5** are strongly quenched in alcohols, even isopropanol. The emission of **4** was not observed in isopropanol, and **3** was quenched more strongly than **5**. Relative quantum yields for all were determined in toluene with anthracene (Φ = 0.30) as a reference. Values for **3**–**6** were determined to be 0.08 ± 0.03, 0.03 ± 0.01, 0.37 ± 0.01,

and 0.43 ± 0.01, respectively. The other quantum yields in Table 1 are based on the toluene value after adjusting for the differences in refractive indices ($n^2_{\text{solvent}}/n^2_{\text{toluene}}$).

3.1.3. Solvato-Chromism

Solvato-chromism in fluorescence spectra can result when the molecular dipole moment of the singlet excited state differs from the ground state due to charge transfer. In acyl naphthylamines, charge transfer occurs from the nitrogen donor to the carbonyl acceptor. As a result, the emission shifts to lower energy as the solvent polarity increases. The magnitude of the solvato-chromism can be determined through plots of the fluorescence maxima vs. the $E_T(30)$ solvent polarity parameter [35] (Figure 4). A steep slope is indicative of strong solvato-chromism. The slopes of the plots for the three ketones are similar in magnitude. The standard deviation of the three slopes is under 10% and the plots for **3** and **5** are nearly coincident. The Stokes shifts for **3**–**5** are 16310, 15370, and 12260 cm^{-1}, respectively, in acetonitrile. The larger shifts for **3** and **4** are a result of their shorter wavelength absorption maxima compared to **5**. The larger shift for **3** vs. **4** is a result of the shorter wavelength emission maximum of **4**. While the absorption maxima for **3** and **4** are very close, the emission of **4** is at shorter wavelengths than **3** for all solvents (Figure 4). Nitrile **6** shows smaller solvato-chromism and emits at shorter wavelengths.
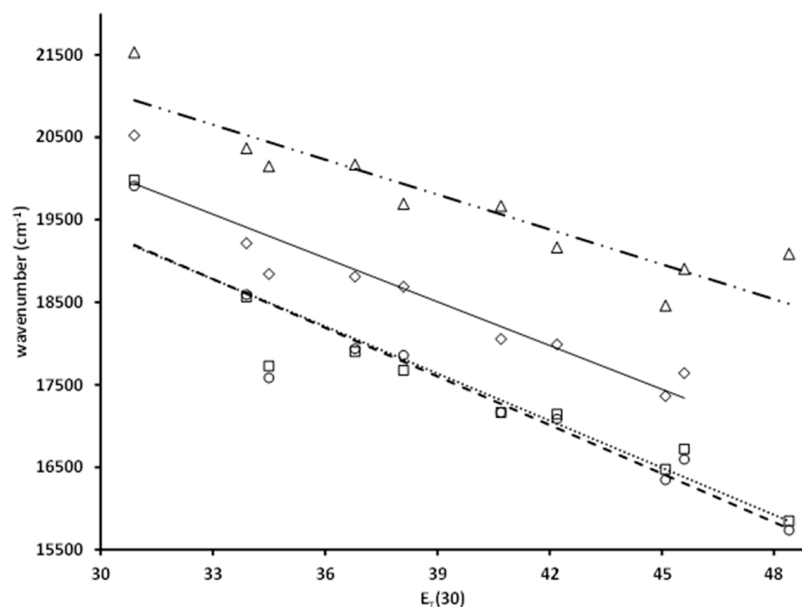

Figure 4. Plots of the emission maxima (cm^{-1}) vs. $E_T(30)$ for **3** ($\bigcirc$), **4** ($\diamondsuit$), **5** ($\square$), and **6** ($\triangle$) in cyclohexane, toluene, chlorobenzene, dichloromethane, ethyl acetate, diethyl ether, acetone, acetonitrile, dimethyl sulfoxide, and isopropanol. Slopes, R^2: -216, 0.96; -177, 0.90; -207, 0.94; -141, 0.83.

3.1.4. Fluorescence Quenching by Protic Solvents

Both 2,6- and 1,5-acyl dialkyl-amino-methyl-amino-naphthalenes show enhanced quenching in protic solvents when the acyl group is twisted out of the naphthalene plane. With the 1,8-derivatives **3** and **4**, the deactivation is so strong that quenching is nearly total. While quenching is also strong with **5**, is it still possible to determine the degree of quenching as a function of the H-bond donating property of the solvent. The plots of the quenching magnitude (log (I_{tol}/I)) vs. the solvent acidity parameter SA [23,24] are fairly linear with a positive slope (Figure 5). The mechanism for quenching is thought to involve H-bond formation from the protic solvent to the carbonyl oxygen in the excited state which leads to an efficient deactivation pathway to the ground state [25]. For context, some 1,5-derivatives show slightly higher slopes (2.7–2.9), but the plots start at lower values (~0.7 vs. 1.1 below). This difference means that H-bonding interactions lead to greater

deactivation in **5** overall, but the sensitivity to a change in the H-bonding donating strength is slightly smaller than the 1,5-derivatives. Nitrile **6** is not quenched by isopropanol.
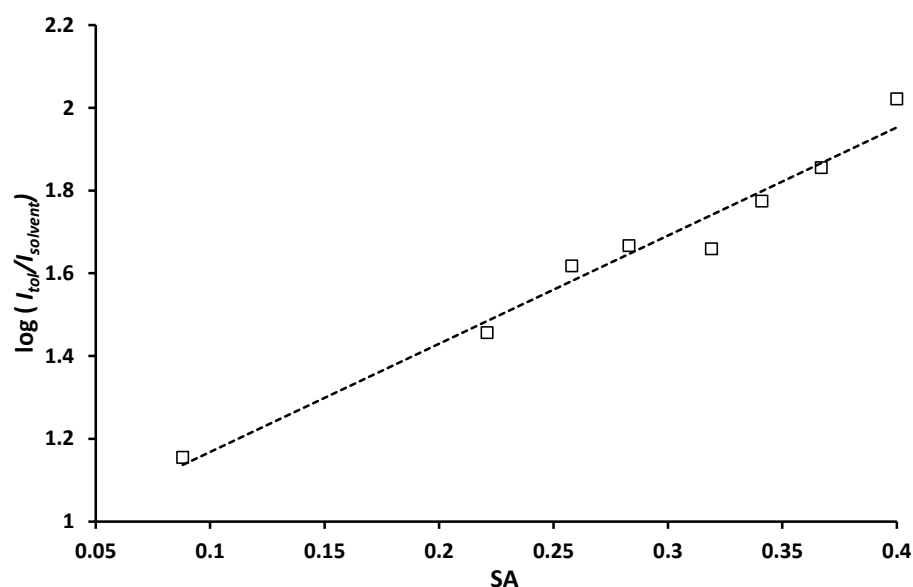

Figure 5. Plot of log (I_{tol}/I) vs. SA for **5** (□). Solvents (SA values): 2-octanol (0.09), 2-butanol (0.22), cyclopentanol (0.26), 2-propanol (0.28), 1-pentanol (0.32), 1-butanol (0.34), 1-propanol (0.37), and ethanol (0.40). Slope, R^2: 2.6, 0.97.

3.2. Computational Studies

The optimized electronic structures for the ground and excited states of **3**–**6** were calculated using Gaussian 16 (DFT, B3YLP, 6311G + 2d,p) [31]. The frontier molecular orbitals of **3**–**6** for the gas phase ground state are shown in Figure 6. Not surprisingly, the HOMO is centered on the nitrogen lone pair for all three. The carbonyl group is a component of the LUMO only with **5**. The nitrile is part of the LUMO with **6**. With **3** and **4** the LUMO is primarily the naphthalene B_{2g} LUMO. The lowest energy singlet excited state (S_1) results from a simple HOMO→LUMO transition.

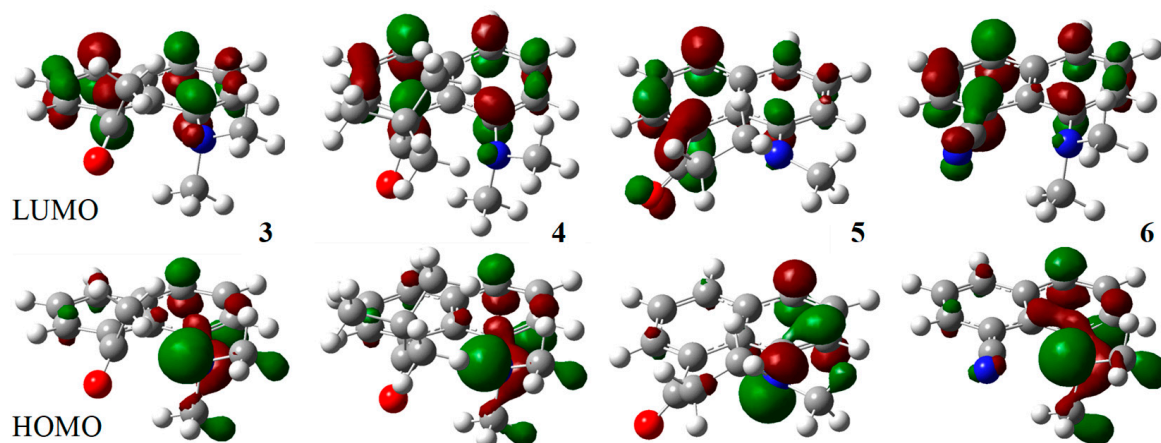**Figure 6.** Calculated frontier molecular orbitals for the gas phase ground states of **3** (**left**), **4** (**middle left**), **5** (**middle right**), and **6** (**right**): LUMO (**top row**), HOMO (**bottom row**).

The optimized ground state and relaxed excited-state structures were also determined using solvent models for toluene and acetonitrile. The frontier molecular orbitals for the relaxed first singlet excited states of **3**–**6** with an acetonitrile model are shown in Figure S1. Toluene and acetonitrile span the mostly linear range of the solvato-chromism plot of

Figure 4. Excluded are cyclohexane, which deviates to higher wavenumbers from the best-fit line, and isopropanol, which is not much more polar than acetonitrile, but significantly quenches the fluorescence. The calculated structures for **3–6** share some common features (Table 2). Several physical values are particularly revealing, especially the degree of twisting of the amino and carbonyl groups and the pyramidalization of the nitrogen atom. The degree of twisting was approximated as the average of the two dihedral angles in Figure 7: d1 and d2 for the carbonyl group and d3 and d4 for the amino group. The degree of pyramidalization of the amino group is indicated by the difference between d3 and d4. In the ground state, the carbonyl groups of **3** and **4** are twisted much more so than **5**, 68° and 78° vs. 46°. The degree of twisting is reduced by a half to a third in the excited states: 21°, 40°, and 18°, respectively. The steric effect of the *tert*-butyl group limits the extent of planarization in the excited state of **4**. The residual twisting results in the higher energy emission of **4** compared with **3** and **5** (Figure 4). The amino groups are significantly pyramidal in the ground state (48°, 50°, 38°, and 48°), but become nearly planar in the excited state (7°, 10°, 2°, and 13°). As with the carbonyl group, the degree of twisting of the amino group is also reduced in the excited state (27°, 25°, and −24°) for **3–5**. For **6** the degree of twisting is slightly reduced (40°) with acetonitrile, but a fully twisted (TICT) state results with toluene (vide infra).

Table 2. Structural features of the calculated ground and excited states of **3–6**.

	State	Solvent	d1	d2	d3	d4	|d3-d4|	C=O [a]	C-N	Q_O [a]	Q_N
					(Degrees)			(Å)		(Mulliken)	
3	S_1	MeCN	19	20	31	24	7	1.26	1.37	−0.56	−0.01
		Tol	21	23	30	24	7	1.26	1.37	−0.50	−0.01
	S_0	MeCN	65	71	85	37	48	1.22	1.43	−0.51	−0.13
		Tol	64	70	82	34	47	1.22	1.43	−0.46	−0.14
4	S_1	MeCN	34	45	30	20	10	1.26	1.37	−0.52	−0.04
		Tol	35	46	30	20	9	1.26	1.37	−0.48	−0.04
	S_0	MeCN	73	84	81	30	51	1.22	1.43	−0.49	−0.11
		Tol	73	84	80	29	50	1.22	1.43	−0.44	−0.12
5	S_1	MeCN	14	25	−25	−22	3	1.26	1.36	−0.58	0.14
		Tol	13	23	−25	−23	2	1.26	1.36	−0.53	0.14
	S_0	MeCN	42	51	−48	−10	38	1.22	1.40	−0.52	−0.02
		Tol	40	49	−48	−11	37	1.22	1.40	−0.47	0.00
6	S_1	MeCN	-	-	47	33	14	1.17	1.38	−0.34	0.02
		Tol	-	-	84	96	12	1.17	1.44	−0.28	0.12
	S_0	MeCN	-	-	78	30	48	1.16	1.42	−0.35	−0.13
		Tol	-	-	77	30	47	1.15	1.41	−0.3	−0.11

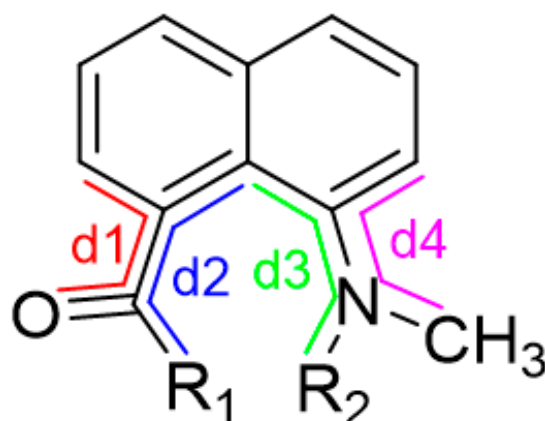[a] For **6**, this is the nitrile bond length and the charge of the nitrile N atom.

Figure 7. Dihedral angles reported in Table 2.

The changes in the C_{aryl}-N and C=O (C≡N) bond lengths along with the charges on the N and O (≡N) atoms between the ground and excited states reflect the intramolecular charge transfer. In all but **6**, the C=O bond elongates and the C_{aryl}-N bond shortens in the excited state. Concomitant with the changes in these bond lengths are an increase of negative charge on the O atom and a decrease of negative charge on the N atom. Nitrile **6** shows the same behavior with acetonitrile, but with toluene, the C_{aryl}-N elongates in the TICT structure, reflecting the lack of partial π-bond formation.

The calculated absorption and emission values with toluene and acetonitrile are shown in Table 3. Both the calculated absorption and emission values are predicted to be at longer wavelengths than the experimental values. All predict relatively small changes in the dipole moment between the ground and relaxed excited states. At first glance, these results stand in contrast to the strong solvato-chromism displayed in Figure 4. The slopes of these plots are very similar to those of the 2,6 and 1,5-prodan regio-isomers [18,20]. Both the 2,6 and 1,5- sets of compounds show larger changes in the dipole moments. A likely explanation for this disparity is that the separation of the donor and acceptor groups is much greater in the 1,5- and 2,6-regioisomers than in the 1,8-derivatives. The solvato-chromism results from the increase in charge more so than the separation of charge (vide infra).

Table 3. Computed emission (em) and absorption (abs) maxima, dipole moments (em: S_1, abs: S_0), and Stokes shifts for **3–6** in toluene (top) and acetonitrile (bottom).

	3		**4**		**5**		**6**	
toluene	em	abs	em	abs	em	abs	em	abs
λ_{max} (nm)	589	333	567	329	574	405	609	396
dipole moment (D)	3.9	3.6	2.9	2.9	4.2	4.1	5.2	4.9
Stokes shift $\times 10^3$ (cm^{-1})	13.1		12.8		7.3		8.8	
acetonitrile								
λ_{max} (nm)	633	332	597	329	614	414	545	396
dipole moment (D)	4.9	4.4	3.7	3.7	5.1	4.9	4.9	5.9
Stokes shift $\times 10^3$ (cm^{-1})	14		14		7.9		6.9	

The calculated Stokes shifts of **5** and **6** are nearly half of those of **3** and **4**. Since the emission maxima of **3** and **5** are almost the same (Figure 4), the smaller shifts for **5** and **6** derive from their longer wavelength absorption maximum, as seen experimentally also. The difference in the absorption maxima for **3** and **5** is due to the difference in their LUMO energies. Twisting in **3** (and **4**) inhibits conjugation between the naphthalene and the carbonyl. In **5** conjugation results in a lower energy LUMO and a lower energy absorption value. The relatively large Stokes shifts for these compounds are a result of the significant changes in the molecular geometry between the ground and excited states. Finally, the formation of the TICT excited state for **6** with toluene stands in contrast to the experimental results. Xu and Liu have found that other TD-DFT methods are better for modeling TICT behavior [36]. These authors, and Chen and Fang, have shown that such TICT states may be non-emissive [10,11,36]. The discrepancy between the experimental and calculated results for **6** will be the subject of future work.

While the calculations predict that the acyl and amino groups of **3–5** twist toward co-planarity in the excited state, they do not reveal whether there is a close-lying TICT state. This point is addressed in **3** using a dihedral angle scan calculation. Starting with the optimized geometry of the S_1 state in acetonitrile, the dihedral angle d4 in Figure 7 is incremented by 5°, and the rest of the geometries are optimized with the 631G + (d) basis set. The results are shown in Figure 8. They suggest that there is a barrier to rotation to form the TICT state.
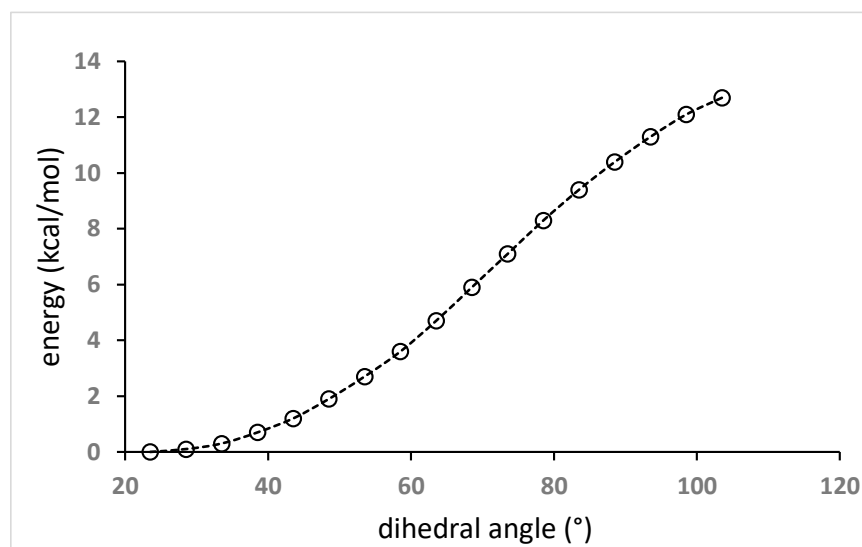
Figure 8. Plot of the relative energy of the optimized excited state of 3 as a function of dihedral angle d4 (Figure 7).

4. Discussion

The proximity of groups attached to the peri positions of naphthalene gives rise to repulsive steric interactions. For **3** and **4**, this effect forces the carbonyl and dimethyl-amino groups to twist out of the plane of the naphthalene ring. In particular, the plane of the carbonyl group is significantly twisted and is nearly perpendicular in **4**. In **5** the groups are tethered together in a seven-membered ring. The carbonyl and amino groups are still twisted with respect to the naphthalene ring, but much less so. This difference in the degree of twisting leads to markedly different absorption maxima for **3** and **4** vs. **5** and results from the poor conjugation of the carbonyl groups in **3** and **4**. In contrast, the emission characteristics of all three are similar. The carbonyl and amino groups are nearly co-planar (~20°) with the naphthalene ring, the amino group itself is nearly planar, the C=O bond is longer, the C_{aryl}-N bond is shorter, and there is partial electron transfer from the N to the O. Because of these common changes, they all show a similar response to solvent polarity. As with other carbonyl-twisted amino naphthalenes, the fluorescence of **3**–**5** is quenched by protic solvents. Because of the greater twisting in **3** and **4**, the quenching is extreme. While the quenching in **5** is very strong, it is still possible to determine the effect of solvent acidity. The magnitude of the quenching is linearly related to the H-bond donating ability of the protic solvent. This result is consistent with a quenching mechanism that involves a H-bonding interaction with the carbonyl group bearing a greater negative charge on the O in the excited state. The nitrile **6** is relatively insensitive to protic solvents. We conclude that for the carbonyl compounds **3**–**5**, despite having twisted ground state geometries, emission occurs from a planar intramolecular charge transfer (PICT) excited state, not a TICT excited state. The unusual computational results with **6** await further investigation.

Author Contributions: Conceptualization, C.A.; methodology, C.A. and K.S.; formal analysis, C.A.; investigation, C.A. and K.S.; data curation, C.A.; writing—original draft preparation, C.A. and K.S.; writing—review and editing, C.A.; supervision, C.A. All authors have read and agreed to the published version of the manuscript.

Conflicts of Interest: The authors declares no conflicts of interest. Kirsten Sweigart's current position at UL Solutions has no relationship to this work.

References

1. Weber, G.; Farris, F.J. Synthesis and Spectral Properties of a Hydrophobic Fluorescent Probe: 6-Propionyl-2-(Dimethylamino) Naphthalene. *Biochemistry* **1979**, *18*, 3075–3078. [CrossRef] [PubMed]
2. Balter, A.; Nowak, W.; Pawekiewicz, W.; Kowalczyk, A. Some Remarks on the Interpretation of the Spectral Properties of Prodan. *Chem. Phys. Lett.* **1988**, *143*, 565–570. [CrossRef]
3. Catalán, J.; Perez, P.; Laynez, J.; Blanco, F.G. Analysis of the Solvent Effect on the Photophysics Properties of 6-Propionyl-2-(Dimethylamino) Naphthalene (PRODAN). *J. Fluoresc.* **1991**, *1*, 215–223. [CrossRef] [PubMed]
4. Kawski, A. Ground-and Excited-State Dipole Moments of 6-Propionyl-2-(Dimethylamino) Naphthalene Determined from Solvatochromic Shifts. *Z. Für Naturforschung A* **1999**, *54*, 379–381. [CrossRef]
5. Samanta, A.; Fessenden, R.W. Excited State Dipole Moment of PRODAN as Determined from Transient Dielectric Loss Measurements. *J. Phys. Chem. A* **2000**, *104*, 8972–8975. [CrossRef]
6. Benedetti, E.; Kocsis, L.S.; Brummond, K.M. Synthesis and Photophysical Properties of a Series of Cyclopenta [b] Naphthalene Solvatochromic Fluorophores. *J. Am. Chem. Soc.* **2012**, *134*, 12418–12421. [CrossRef] [PubMed]
7. Jockusch, S.; Zheng, Q.; He, G.S.; Pudavar, H.E.; Yee, D.J.; Balsanek, V.; Halim, M.; Sames, D.; Prasad, P.N.; Turro, N.J. Two-Photon Excitation of Fluorogenic Probes for Redox Metabolism: Dramatic Enhancement of Optical Contrast Ratio by Two-Photon Excitation. *J. Phys. Chem. C* **2007**, *111*, 8872–8877. [CrossRef]
8. Brummond, K.M.; Kocsis, L.S. Intramolecular Didehydro-Diels–Alder Reaction and Its Impact on the Structure–Function Properties of Environmentally Sensitive Fluorophores. *Acc. Chem. Res.* **2015**, *48*, 2320–2329. [CrossRef]
9. Grabowski, Z.R.; Rotkiewicz, K.; Rettig, W. Structural Changes Accompanying Intramolecular Electron Transfer: Focus on Twisted Intramolecular Charge-Transfer States and Structures. *Chem. Rev.* **2003**, *103*, 3899–4031. [CrossRef]
10. Wang, C.; Chi, W.; Qiao, Q.; Tan, D.; Xu, Z.; Liu, X. Twisted Intramolecular Charge Transfer (TICT) and Twists beyond TICT: From Mechanisms to Rational Designs of Bright and Sensitive Fluorophores. *Chem. Soc. Rev.* **2021**, *50*, 12656–12678. [CrossRef]
11. Chen, C.; Fang, C. Fluorescence Modulation by Amines: Mechanistic Insights into Twisted Intramolecular Charge Transfer (TICT) and Beyond. *Chemosensors* **2023**, *11*, 87. [CrossRef]
12. Kochman, M.A.; Durbeej, B. Simulating the Nonadiabatic Relaxation Dynamics of 4-(N, N-Dimethylamino) Benzonitrile (DMABN) in Polar Solution. *J. Phys. Chem. A* **2020**, *124*, 2193–2206. [CrossRef] [PubMed]
13. Okada, T.; Uesugi, M.; Köhler, G.; Rechthaler, K.; Rotkiewicz, K.; Rettig, W.; Grabner, G. Time-Resolved Spectroscopy of DMABN and Its Cage Derivatives 6-Cyanobenzquinuclidine (CBQ) and Benzquinuclidine (BQ). *Chem. Phys.* **1999**, *241*, 327–337. [CrossRef]
14. Köhler, G.; Rechthaler, K.; Grabner, G.; Luboradzki, R.; Suwińska, K.; Rotkiewicz, K. Structure of Cage Amines as Models for Twisted Intramolecular Charge-Transfer States. *J. Phys. Chem. A* **1997**, *101*, 8518–8525. [CrossRef]
15. Wermuth, G.; Rettig, W. The Interaction of Close-Lying Excited States: Solvent Influence on Fluorescence Rate and Polarization in Substituted Indolines. *J. Phys. Chem.* **1984**, *88*, 2729–2735. [CrossRef]
16. Rotkiewicz, K.; Rubaszewska, W. Intramolecular Charge Transfer State and Unusual Fluorescence from an Upper Excited Singlet of a Nonplanar Derivative of P-Cyano-N, N-Dimethylaniline. *J. Lumin.* **1982**, *27*, 221–230. [CrossRef]
17. Anderson, R.S.; Nagirimadugu, N.V.; Abelt, C.J. Fluorescence Quenching of Carbonyl-Twisted 5-Acyl-1-Dimethylaminonaphthalenes by Alcohols. *ACS Omega* **2019**, *4*, 14067–14073. [CrossRef]
18. Chen, T.; Lee, S.W.; Abelt, C.J. 1,5-Prodan Emits from a Planar Intramolecular Charge-Transfer Excited State. *ACS Omega* **2018**, *3*, 4816–4823. [CrossRef]
19. Davis, B.N.; Abelt, C.J. Synthesis and Photophysical Properties of Models for Twisted PRODAN and Dimethylaminonaphthonitrile. *J. Phys. Chem. A* **2005**, *109*, 1295–1298. [CrossRef]
20. Everett, R.K.; Nguyen, H.A.A.; Abelt, C.J. Does PRODAN Possess an O-TICT Excited State? Synthesis and Properties of Two Constrained Derivatives. *J. Phys. Chem. A* **2010**, *114*, 4946–4950. [CrossRef]
21. Lobo, B.C.; Abelt, C.J. Does PRODAN Possess a Planar or Twisted Charge-Transfer Excited State? Photophysical Properties of Two PRODAN Derivatives. *J. Phys. Chem. A* **2003**, *107*, 10938–10943. [CrossRef]
22. Kiefl, C. Correlated Rotations and Unusual Fluorescence Properties of peri-Substituted, Axially Chiral Naphthyl Ketones. *Eur. J. Org. Chem.* **2000**, *2000*, 3279–3286. [CrossRef]
23. Gallucci, J.C.; Hart, D.J.; Young, D.G.J. Nucleophile–Electrophile Interactions in 1,8-Disubstituted Naphthalenes: Structures of Three 1-Naphthaldehydes and a 1-Naphthyl Methyl Ketone. *Acta Crystallogr. B* **1998**, *54*, 73–81. [CrossRef]
24. Schweizer, W.B.; Procter, G.; Kaftory, M.; Dunitz, J.D. Structural Studies of 1,8-Disubstituted Naphthalenes as Probes for nucleophile-electrophile interactions. *Helv. Chim. Acta* **1978**, *61*, 2783–2808. [CrossRef]

25. Bulgarevich, S.B.; Ivanova, N.A.; Movshovich, D.Y.; Mannschreck, A.; Kiefl, C. Conformational Investigation of 1,8-Disubstituted Naphthalenes as Solutes by Kerr Effect and Dipole Moment Methods. *J. Mol. Struct.* **1994**, *326*, 17–24. [CrossRef]

26. Hodgson, D.R.W.; Kirby, A.J.; Feeder, N. The Case of the Missing Acetylene. The Mechanism of an Intramolecular SN(V) Reaction and a New Route to 1-Methylbenzo[de]Quinolines. *J. Chem. Soc. Perkin 1* **1999**, *1*, 949–954. [CrossRef]

27. Clayden, J.; McCarthy, C.; Helliwell, M. Bonded Peri-Interactions Govern the Rate of Racemisation of Atropisomeric 8-Substituted 1-Naphthamides. *Chem. Commun.* **1999**, *20*, 2059–2060. [CrossRef]

28. Noyes, W.A. *n*-BUTYL NITRITE. *Org. Synth.* **1936**, *16*, 7. [CrossRef]

29. Vogel, A.I. *A Text-Book of Practical Organic Chemistry Including Qualitative Organic Analysis*, 3rd ed.; Longmans: London, UK, 1974; ISBN 978-0-582-44245-0.

30. Lakowicz, J.R. *Principles of Fluorescence Spectroscopy*; Springer: Boston, MA, USA, 1999; ISBN 978-1-4757-3063-0.

31. Frisch, M.M.J.; Trucks, G.W.; Schlegel, H.B.; Scuseria, G.E.; Robb, M.A.; Cheeseman, J.R.; Scalmani, G.; Barone, V.; Petersson, G.A.; Nakatsuji, H.; et al. *Gaussian 16, Version 1.1*; Gaussian, Inc.: Wallingford, CT, USA, 2016.

32. Kirby, A.J.; Percy, J.M. Synthesis of 8-Substituted 1-Naphthylamine Derivatives. Exceptional Reactivity of the Substituents. *Tetrahedron* **1988**, *44*, 6903–6910. [CrossRef]

33. Kiefl, C.; Mannschreck, A. 1,8-Disubstituted Naphthalenes by Directed Metalation and Subsequent Lithium-Manganese Exchange, Including Copper Catalysis. *Synthesis* **1995**, *1995*, 1033–1037. [CrossRef]

34. Lum, K.; Zielinski, S.M.; Abelt, C.J. Dansyl Emits from a PICT Excited State. *J. Phys. Chem. A* **2021**, *125*, 1229–1233. [CrossRef] [PubMed]

35. Reichardt, C.; Welton, T. *Solvents and Solvent Effects in Organic Chemistry*; Wiley-VCH Verlag GmbH: Weinheim, Germany, 2011.

36. Wang, C.; Qiao, Q.; Chi, W.; Chen, J.; Liu, W.; Tan, D.; McKechnie, S.; Lyu, D.; Jiang, X.; Zhou, W.; et al. Quantitative Design of Bright Fluorophores and AIEgens by the Accurate Prediction of Twisted Intramolecular Charge Transfer (TICT). *Angew. Chem. Int. Ed.* **2020**, *59*, 10160–10172. [CrossRef] [PubMed]